

UPDATING SOIL SURFACE CONDITIONS DURING WIND EROSION EVENTS USING THE WIND EROSION PREDICTION SYSTEM (WEPS)

L. J. Hagen

ABSTRACT. *During significant wind erosion events, the soil surface is continually modified; however, erosion models rarely account for these changes. The objectives of this work are to provide an overview of the WEPS soil surface update methodology and demonstrate that by periodic surface updating during events, a physically based, field-scale model can (1) improve prediction accuracy and (2) determine changes in erosion control by clods, crusts, and soil roughness, so model users can improve their designs. During wind erosion events, the soil surface can become armored. This represents a supply-limited condition and is typical of the upwind portions of a field. Conversely, when additional mobile soil is created or uncovered faster than it is removed, the surface becomes more erodible, as often occurs on the downwind portions of large fields. In this case, soil removal may be limited by the duration of the erosive winds. To facilitate surface updating in WEPS, a mass balance of the available mobile soil is maintained in two pools: one for the mobile soil on the crust, and another for the mobile soil among the immobile aggregates. The net emission of the mobile aggregates is simulated in grid cells along the wind direction, and the pools in each cell are updated on a subhourly basis. Partial depletion of a pool may cause cessation of erosion at a given wind speed, but permit erosion to resume at succeeding higher wind speeds. During an event, random roughness, oriented roughness, and the fraction of mobile aggregate cover are also updated. In contrast to models that limit erosion only by storm duration, surface updating increased WEPS accuracy both by identifying field areas that limited supply of mobile aggregates and by changing threshold friction velocities to allow simulation of intermittent erosion.*

Keywords. *Model, Soil, Wind erosion.*

During wind erosion, the downwind increase in the soil discharge (fetch effect) has long been observed (Chepil, 1946), but rigorous explanations for the phenomenon are more recent. Gillette et al. (1996) suggested that three processes contributed to the fetch effect: avalanching, in which a saltating aggregate impacts the surface and sets additional mobile aggregates in motion; aerodynamic feedback, in which an increase in saltating aggregates increases the apparent aerodynamic surface roughness; and surface modifications, which change the threshold wind speeds. They concluded that surface modifications were the major mechanism causing field-scale fetch effects.

Short-term intermittent saltation has been ascribed to variations in the wind strength (Stout and Zobeck, 1997). Longer-term variations in soil discharge during a storm may be ascribed to variations in both wind speed and surface conditions. When the potential soil discharge is significantly reduced or even ceases during a wind storm, the effect is often

described as a “supply-limited” surface condition (Mansell et al., 2006; Gillette and Chen, 2001; Okin and Gillette, 2004). When crusts are destroyed, the supply of mobile aggregates exposed at the surface is generally increased (Chepil, 1958; Gillette et al., 2001).

Crusts and immobile aggregates serve as strong modulators of wind erosion (Chepil and Woodruff, 1963; Goossens, 2004). The strength of crusts and aggregates depends on both the formation processes and the soil composition (Chepil and Woodruff, 1963; Skidmore and Layton, 1992). The breakdown of crusts and aggregates by abrasion depends on their strength and the abrader discharge rate (Hagen, 1991b; Hagen et al., 1992; Zobeck, 1991).

In erosion models such as WEQ (Woodruff and Siddoway, 1965), WEPS (Hagen, 1991a), SEEM (Fryrear et al., 1998), the soil surface is typically assumed to be relatively uniform at the beginning of erosion events. But as significant wind erosion occurs on agricultural fields, the erosion processes continually modify the field surface along the downwind direction during the storm (Hagen et al., 1999). These surface modifications often include removing the mobile soil near the upwind, non-erodible boundary or from tillage ridge tops, so the surface becomes armored. Meanwhile downwind, the entrainment of mobile soil and the creation of new mobile soil by abrasion of immobile clods or crust enable saltation/creep-size aggregates to approach the wind transport capacity. Where discharge is at transport capacity, the creation of additional mobile soil by abrasion continues and causes a net increase of the saltation/creep-size soil on the surface. In contrast, the transport capacity for suspension-size aggregates

Submitted for review in July 2007 as manuscript number SW 7111; approved for publication by the Soil & Water Division of ASABE in November 2007. Presented at the 2007 ASABE Annual Meeting as Paper No. 072257.

Contribution from the USDA-ARS in cooperation with the Kansas Agricultural Experiment Station. Contribution No. 07-278-J from the Kansas Agricultural Experiment Station, Manhattan, Kansas.

The author is **Lawrence J. Hagen, ASABE Member Engineer**, Agricultural Engineer, Wind Erosion Research Unit, USDA-ARS Grain Marketing and Production Research Center, 1515 College Ave, Manhattan, Kansas 66502; phone: 785-537-5545; e-mail: hagen@weru.ksu.edu.

Table 1. Surface conditions updated during erosion.

Symbol	Definition	Units
SM_{los}	Soil mobile mass on crusted surface	kg m ⁻²
SF_{cr}	Soil fraction of surface crust cover	m ² m ⁻²
SF_{los}	Soil fraction loose cover on crust	m ² m ⁻²
SZ_{cr}	Soil depth of crust (consolidated zone)	mm
$SMag_{los}$	Soil mobile mass on aggregated surface	kg m ⁻²
SF_{84}	Soil mass fraction <0.84 mm on aggregated surface, and mobile cover fraction on aggregated surface	kg kg ⁻¹ m ² m ⁻²
SF_{200}	Soil mass fraction <2.00 mm on aggregated surface	kg kg ⁻¹
SF_{10}	Soil mass fraction <0.1 mm on aggregated surface	kg kg ⁻¹
SV_{roc}	Soil volume rock >2.0 mm diameter	m ³ m ⁻³
SZ_{rg}	Ridge height	mm
SL_{rr}	Random roughness height (standard deviation)	mm

(dust) is so large that creation and entrainment of dust generally occurs over all eroding portions of a field. The unrestricted sorting and removal of the dust leads to many off-site problems (Wagner and Hagen, 2001) as well as soil degradation on some soil textures (Lyles and Tatarko, 1986).

From the preceding evidence, it appears useful to update the surface during significant wind erosion events in order to properly simulate fetch effects, intermittent erosion, and surface armoring and to distinguish between supply limited and unlimited erosion events. Hence, the objectives of this article are to provide an overview of the surface updating methodology used in the WEPS model and to demonstrate that by periodic updating of soil surface conditions during events, a physically based field-scale model can (1) improve accuracy of its predictions and (2) determine changes in erosion control by clods, crusts, and soil roughness, so model users can improve their designs.

THEORY

For wind erosion simulation, the field-scale region is divided into rectangular grid cells. The surface conditions in all the cells are periodically updated using variable time-steps that range from 0.6 to 30 min depending upon erosion rates. Variable time-steps were used to minimize simulation run time. The surface conditions updated are summarized in table 1.

In general, few field measurements are available to validate the simulated response of field surface conditions to erosion. Hence, simple equations based on mass balance in the surface layer were developed to estimate changes in the surface represented by each grid cell.

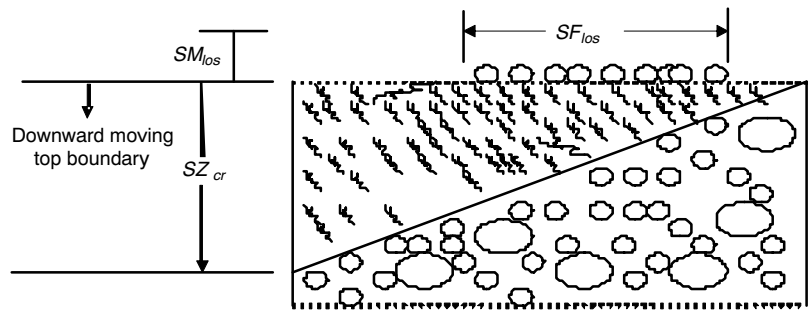


Figure 1. Schematic of triangular-shaped consolidated zone (crust) with depth (SZ_{cr}) overlying an aggregated soil and having a mobile cover fraction (SF_{los}) with a mass (SM_{los}).

CHANGE IN MOBILE SURFACE SOIL MASS

Solutions to the WEPS sediment transport equations (Hagen et al., 1999) are used to estimate the net addition (+) or loss (-) of mobile aggregates during a time interval (Δt) over a length segment (Δx) of a grid cell as:

$$dmt_{los} = \left[\frac{-(q_0 - q_i) - (qss_0 - qss_i)}{\Delta x} \right] \Delta t + F_{an} C_{an} q_i \Delta t \quad (1)$$

where

dmt_{los} = net change in mobile soil surface aggregates during time interval Δt (kg m⁻²)

q_0 = horizontal saltation/creep soil discharge out of a grid cell (kg m⁻¹ s⁻¹)

q_i = horizontal saltation/creep soil discharge into a grid cell (kg m⁻¹ s⁻¹)

qss_0 = horizontal suspended soil (dust) discharge out of a grid cell (kg m⁻¹ s⁻¹)

qss_i = horizontal suspended soil (dust) discharge into a grid cell (kg m⁻¹ s⁻¹)

F_{an} = mass fraction of q_i impacting immobile clods and crust

C_{an} = coefficient of abrasion of immobile clods and crust (m⁻¹).

The first term represents loss or gain by erosion, and the second term represents creation of new mobile aggregates by the abrasion process.

Two reservoirs of mobile soil may be present at the soil surface. These include mobile soil on a consolidated surface, hereafter called crusted, and mobile soil among the rock and immobile aggregates. Because these reservoirs differ in both creation processes and their response to erosion, they are updated separately.

UPDATE OF CRUSTED SURFACE

Undisturbed, crusted soil surfaces have high threshold wind speeds and are generally stable, unless abraded by mobile soil aggregates (Gillette, 1982; Langston and McKenna Neuman, 2005). Crusts are complex because there are spatial variations in crust thickness and resistance to abrasion as well as preferential zones for abrader impact caused by the surface micro-topography. Nevertheless, in WEPS, the surface within each grid cell is assumed to be homogeneous, and the crust depth is simulated as a triangular shape (fig. 1). Hence, uniform abrasion of the crust continually exposes an increasing area of aggregated soil to the surface wind stress.

The deflatable reservoir of mobile soil on the crusted surface is regarded as a constant for all friction velocities above threshold. Hence, it is updated as:

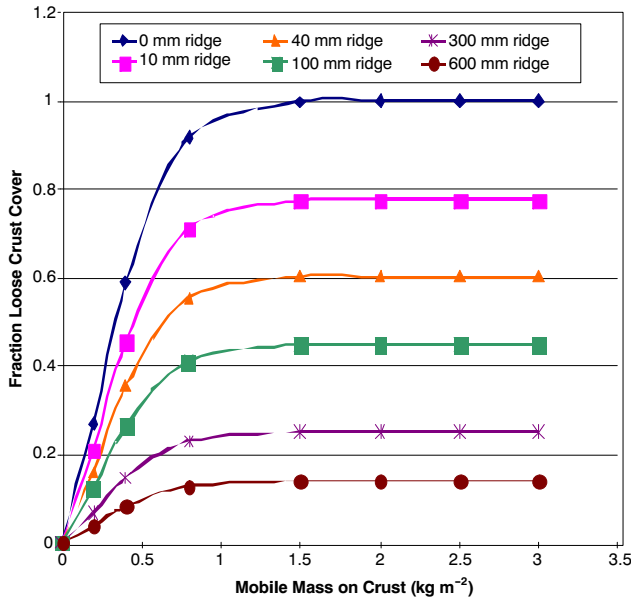


Figure 2. Loose, mobile cover of aggregates on crust as a function of mobile mass for a range of ridge heights.

$$SM_{los} = SM_{los0} + dm_{t_{los}} \quad (2)$$

where

SM_{los} = mobile soil aggregates per unit area of the crusted surface (kg m^{-2})

SM_{los0} = value of SM_{los} at prior time-step (kg m^{-2}).

If either the crusted or aggregated mobile soil reservoirs cannot supply the simulated soil loss per unit area from their area of surface coverage, then the additional soil loss is removed from the remaining reservoir. When neither reservoir can supply the demand, emission from a given grid cell ceases until additional mobile soil is deposited.

Updated values of the mobile aggregate mass on the crusted surface are used to update the fraction of mobile crust cover as:

$$SF_{los} = [1 - \exp(-3.5SM_{los}^{1.5})]CR_{los} \quad (3)$$

The layer thickness of mobile aggregate deposits tends to increase with surface roughness. Hence, the coefficient CR_{los} reduces mobile cover as surface roughness increases, and is estimated as:

$$CR_{los} = \exp(-0.08SZ^{0.5}) \quad (4)$$

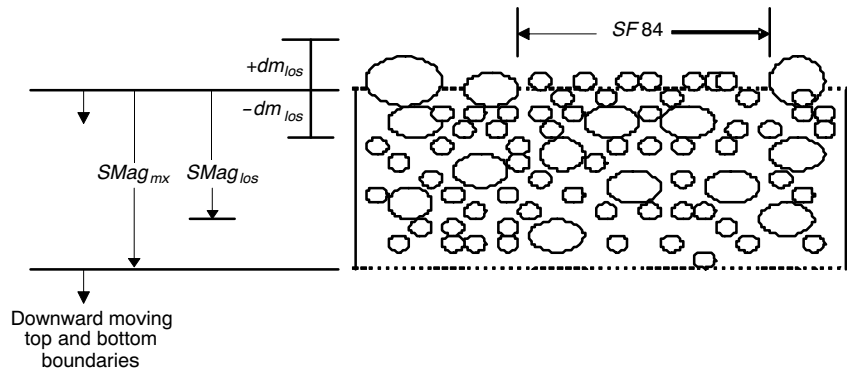


Figure 3. Schematic of the aggregated surface with mobile cover (SF_{84}) and additions or depletions to the mobile mass ($\pm dm_{los}$).

and

$$SZ = \max(SZ_{rg}, 4SL_{rr}) \quad (5)$$

where

SZ_{rg} = ridge height (mm)

SL_{rr} = random roughness (mm).

Mobile aggregate cover on a crusted surface is a function of mobile mass modified by surface roughness, as illustrated for ridge height levels in figure 2.

Crust thickness is reduced by abrasion on the crust and is simulated as:

$$SZ_{cr} = SZ_{cr0} - \left(\frac{Fan_{cr0}Can_{cr}q_i}{1.4SF_{cr0}} \right) \Delta t, \quad SF_{cr0} > 0.01 \quad (6)$$

where

SZ_{cr} = updated crust thickness (mm)

SZ_{cr0} = crust thickness at prior time-step (mm)

Fan_{cr0} = fraction abraded impacting bare crust surface at prior time-step

Can_{cr} = coefficient of crust abrasion (m^{-1})

SF_{cr0} = Surface fraction crust at prior time-step.

Finally, crust cover is updated in proportion to crust thickness as:

$$SF_{cr} = SF_{cr0} \frac{SZ_{cr}}{SZ_{cr0}} \quad (7)$$

where SF_{cr} = is updated crust cover fraction.

UPDATE OF AGGREGATED SURFACE

On aggregated surfaces, some of the mobile material is typically sheltered by micro-roughness of the immobile aggregates. Hence, the reservoir of mobile material available for deflation varies with friction velocity. Before updating the fraction of mobile mass (SF_{84}) in the surface layer reservoir, it is necessary to define that reservoir. In this model, the initial reservoir ($SMag_{mx}$) is defined as the maximum mass of mobile soil that could be removed under a high friction velocity from a bare, smooth soil containing the initial aggregate mixture. The actual removable soil under a lowered friction velocity and other surface conditions is $SMag_{los}$, as illustrated in figure 3.

The mobile aggregate cover fraction on the aggregated surface is assumed to equal the mass fraction, SF_{84} . The initial aggregated mixture is assumed to be uniform with depth. Hence, as erosion lowers the soil surface, the top and bottom boundaries move downward so that the reservoir layer involved with erosion that was initially defined by $SMag_{mx}$ re-

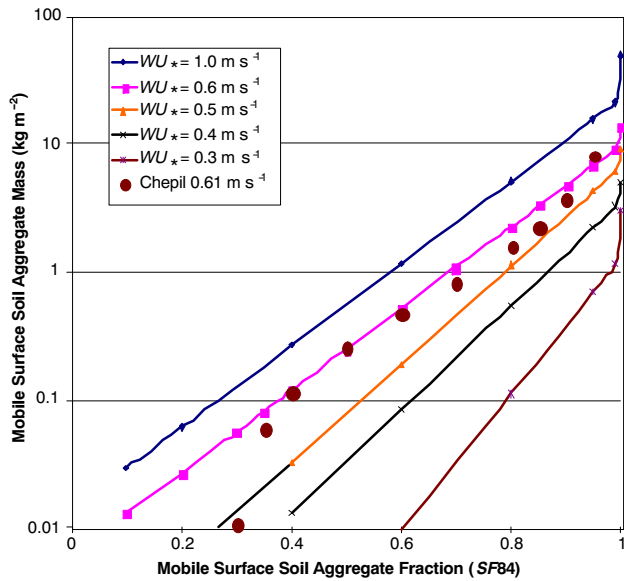


Figure 4. Simulated mass of mobile aggregates that can be removed from flat, bare aggregated surface for a range of friction velocities with average measured data at friction velocity of 0.61 m s^{-1} (Chepil, 1958).

mains constant. The net mass of mobile soil removed (-) or added (+) to the reservoir is dm_{los} . When mobile soil deposition exceeds $SMag_{mx}$, the reservoir of potentially mobile soil is increased.

To simulate the aggregated surface, the cumulative change of mass of mobile material is updated as:

$$dm_{los} = dm_{los0} + dmt_{los} \quad (8)$$

where

dm_{los} = cumulative mobile soil loss or gain on aggregated surface (kg m^{-2})

dm_{los0} = value of dm_{los} at prior time-step.

When $dm_{los} < 0$, mobile soil is removed from the initial soil reservoir among the immobile aggregates. Based on wind tunnel measurements (Chepil, 1951, 1958; Hagen, 1991b), empirical relationships (fig. 4) were developed to estimate the mass of mobile aggregates that could be removed from a flat, bare, aggregated surface. The surfaces were characterized by the initial mass fractions of mobile aggregates $< 0.84 \text{ mm}$ diameter ($SF84_{ic}$) and tested for a range of friction velocities without abraded.

The maximum removable mass in the mobile reservoir was estimated at a friction velocity (WU^*) of 0.75 m s^{-1} for a bare, smooth, aggregated surface as:

$$SMag_{mx} = \exp[2.708 - 7.603 \times \{(1 - SF84_{ic})(1 - SVroc_{ic}) + SVroc_{ic}\}] \quad (9)$$

The total soil mass in the reservoir of the affected layer is then estimated as:

$$SM_{tot} = \frac{SMag_{mx}}{SF84_{ic}(1.001 - SVroc_{ic})} \quad (10)$$

The maximum reservoir is reduced by roughness, residue cover, and wetness, so an estimate the available mobile reservoir at the current friction velocity is:

$$SMag_{los} = SMag_{mx} \frac{WU^* - WU_{*t}}{0.75 - WU_{*t}}, \quad SMag_{los} \geq 0 \quad (11)$$

$$WU_{*t0} = 1.7 - 1.35 \exp[0.07834 - 0.3261 \times \{(1 - SF84_{ic})(1 - SVroc_{ic}) + SVroc_{ic}\}^2],$$

$$SF84_{ic} > 0.0 \quad (12)$$

where

WU_{*t0} = threshold friction velocity for bare, aggregated, smooth soil (m s^{-1})

WU_{*t} = threshold friction velocity for the current cell surface (m s^{-1}).

When the soil removal from the reservoir at the current friction velocity equals $SMag_{los}$, the mobile soil fraction ($SF84_{mn}$) still remaining in the maximum mobile soil reservoir is:

$$SF84_{mn} = \frac{(SMag_{mx} - SMag_{los})}{SM_{tot}} \quad (13)$$

When there is net soil mass removal from the aggregated reservoir ($dm_{los} < 0$), $SF84$ is updated as:

$$SF84 = \frac{SMag_{mx} + dm_{los}}{SM_{tot}} \quad (14)$$

In any grid cell, when $SF84 \leq SF84_{mn}$ emission of mobile soil ceases from that cell.

When there is net deposition ($dm_{los} > 0$), the immobile surface aggregates can become slowly buried by the addition of mobile soil to the initial reservoir. The total mass in the initial reservoir (SM_{tot}) is now increased by the amount dm_{los} . In this case, the surface fraction of mobile aggregates is adjusted upward and updated as:

$$SF84 = \frac{SMag_{mx} + dm_{los}}{SM_{tot} + dm_{los}} \quad (15)$$

UPDATE OF OTHER SOIL FRACTIONS

The soil fraction $< 2.0 \text{ mm}$ in diameter ($SF200$) is estimated from the values of the soil fraction $< 0.84 \text{ mm}$ in diameter ($SF84$) as:

$$SF200 = (2 - SF84)SF84 \quad (16)$$

If $dm_{los} < 0.0$, then the suspension-size soil fraction $< 0.1 \text{ mm}$ in diameter ($SF10$) is updated in proportion to the updated $SF84$ as:

$$SF10 = SF10_{ic} \frac{SF84}{SF84_{ic} + 0.001} \quad (17)$$

where

$SF10_{ic}$ = is the $SF10$ initial condition at the beginning of the erosion event

$SF84_{ic}$ = is the $SF84$ initial condition at the beginning of the erosion event.

When there is mobile soil gain at the soil surface, the suspension-size aggregates $< 0.10 \text{ mm}$ diameter ($SF10$) tend to be sorted out of the depositing soil. Hence, for $dm_{los} > 0.0$, the estimate is:

Table 2. Simulation run treatment summary.

Surface Conditions	Storm Wind Speed Distribution		
	Max. Wind Middle	Max. Wind First	Max. Wind Last
Bare, aggregated, updated	X	X	X
Bare, crusted, updated	X		
Flat cover, aggregated, updated	X		
Flat cover, crusted, updated	X		
Bare, aggregated, no update	X		

$$SF10 = \frac{SF10_{ic} SM_{tot}}{SM_{tot} + dmt_{los}} \quad (18)$$

UPDATE OF SURFACE ROCK VOLUME

The rocks (>2.0 mm diameter) are assumed to be mixed with the soil and have a uniform vertical distribution. If an initial desert pavement is present, the surface is generally assumed to be stable. Surface rock volume increases or decreases in proportion to the deflation or deposition from the surface area that is not covered by rock and is estimated to slowly change for rock with a wide size distribution as:

$$SV_{roc} = SV_{roc0} - \frac{7.5dmt_{los}}{1200(1 - SV_{roci})} \quad (19)$$

where

- SV_{roc} = soil rock volume ($m^3 m^{-3}$)
- SV_{roc0} = soil rock volume at prior time-step ($m^3 m^{-3}$)
- SV_{roci} = soil rock volume at initial time-step ($m^3 m^{-3}$).

UPDATE SURFACE ROUGHNESS

Roughness elements consist of random roughness and, if present, oriented roughness such as tillage ridges. The first step in updating roughness is estimating the effects of changes in loose soil depth generated by the various erosion processes.

When the soil surface has roughness elements that actively trap saltation-size aggregates, net deposition ($dmt_{los} > 0$) of mobile soil in sheltered areas decreases roughness height, SZ_v (mm) as:

$$SZ_v = \frac{-2.0dmt_{los}}{1.2} \quad (20)$$

When saltation trapping occurs, but with a net loss ($dmt_{los} < 0$) from both sheltered and unsheltered areas, roughness height slowly decreases as:

$$SV_v = \frac{dmt_{los}}{1.2} \quad (21)$$

When the soil surface is relatively smooth, i.e., random roughness < 10.0 mm and ridge roughness < 50.0 mm, then net deposition ($dmt_{los} > 0$) over much of the area decreases roughness height as:

$$SZ_v = \frac{-dmt_{los}}{1.2} \quad (22)$$

While net loss with smooth conditions slowly increases roughness as:

$$SZ_v = \frac{0.5dmt_{los}}{1.2} \quad (23)$$

The change in roughness height caused by abrasion of immobile clods and crust is:

$$SZ_{an} = \frac{-2.0(F_{an} C_{an} q_i) \Delta t}{1.4} \quad (24)$$

Total roughness height change, SZ_t (mm) is:

$$SZ_t = SZ_v + SZ_{an} \quad (25)$$

Ridge height is updated as:

$$SZ_{rg} = SZ_{rg0} + SZ_t, \quad SZ_{rg} \geq 0 \quad (26)$$

where

- SZ_{rg} = ridge height (mm)
- SZ_{rg0} = ridge height at prior time-step (mm).
- Random roughness is updated as:

$$SL_{rr} = SL_{rr0} \frac{SZ_t}{4.0}, \quad SL_{rr} \geq 1.5 \quad (27)$$

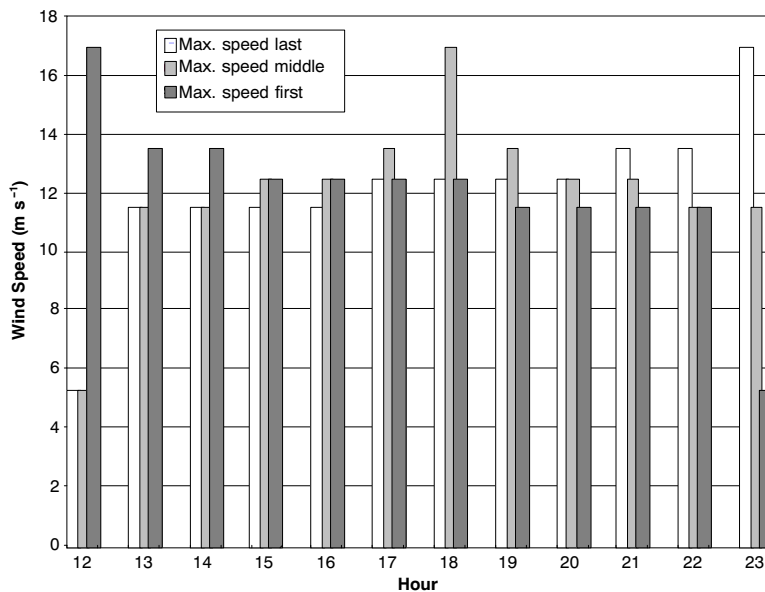


Figure 5. Three variations of the sequence in wind speeds for the single erosive wind energy used in the simulation runs.

Table 3. Soil and initial condition inputs to WEPS Erosion submodel for bare aggregated or crusted soils with and without flat residue cover.

Parameter	Units	Amarillo	Colby
		Fine Sandy Loam	Silt Loam
Intrinsic soil properties			
Sand	Mg Mg ⁻¹	0.66	0.095
Fine sand	Mg Mg ⁻¹	0.16	0.067
Silt	Mg Mg ⁻¹	0.20	0.68
Clay	Mg Mg ⁻¹	0.14	0.225
Rock volume	m ³ m ⁻³	0.0	0.0
1.5 mPa water content	Mg Mg ⁻¹	0.09	0.125
Top soil layer depth	mm	330	330
Temporal soil clod parameters			
Geometric mean diameter	mm	2.35	5.60
Geometric std. dev.	mm mm ⁻¹	12.6	15.2
Maximum diameter	mm	32.5	37.8
Minimum diameter	mm	0.01	0.01
Dry stability	ln(J kg ⁻¹)	2.56	3.16
Density	Mg Mg ⁻¹	1.60	1.60
Temporal crust properties			
Crust depth	mm	0, 5.86	0, 5.45
Crust density	Mg Mg ⁻¹	0, 1.4	0, 1.4
Crust cover	m ² m ⁻²	0, 0.97	0, 0.97
Crust loose cover	m ² m ⁻²	0, 0.6	0, 0.4
Crust loose cover mass	kg m ⁻²	0, 0.8	0, 0.6
Crust dry stability	ln(J kg ⁻¹)	0, 2.35	0, 3.16
Temporal surface roughness			
Random roughness	mm	6.0, 3.6	6.0, 4.1
Ridge height	mm	0.0	0.0
Ridge spacing	mm	0.0	0.0
Ridge orientation	degrees	0.0	0.0
Biomass cover			
Flat residue	m ² m ⁻²	0.0, 0.15	0.0, 0.15
Field length			
Strip	m	100	100
Small size	m	200	200
Medium size	m	400	400
Large size	m	800	800

where

SL_{rr} = random roughness (mm)

$SL_{rr 0}$ = random roughness at prior time-step (mm).

WEPS EROSION SIMULATION INPUTS

For these simulations, two soil series, an Amarillo fine sandy loam and a Colby silt loam, were selected. An initial

bare, aggregated surface was simulated along with three different treatments to enable comparisons among the soil losses. Treatments included a crusted surface caused by 75 mm of rainfall that reduced soil roughness, and a 0.15 flat residue cover on both the aggregated and crusted surfaces. In the final simulation, surface updating was disabled, so the initial aggregated, bare, soil surface was maintained throughout the duration of the windstorm (table 2).

The WEPS wind speed simulator generates daily windstorms with a symmetrical shape with the maximum wind speeds near the middle of each storm. In these simulations, a single 11 h storm with a symmetrical wind speed distribution was used for all surface treatments. To observe the effects of non-symmetric speed distributions on the bare, aggregated surfaces, the sequence of the storm wind speeds was varied, so the maximum wind speeds were at the beginning or end of the storm. The three wind speed variations all have equal wind energies and are illustrated in figure 5. The surface simulation input parameters to the WEPS Erosion submodel are quantified in table 3.

RESULTS AND DISCUSSION

The simulated soil losses at the end of each windstorm are summarized in table 4. Soil loss from the bare, aggregated surfaces decreased dramatically as field length decreased. This effect is mainly attributed to the reductions in both the amount of available saltation-size material available for abrasion and the length of area available for the abraded to cross. The surfaces also lacked substantial sheltered areas, such as tillage ridges, for trapping the abraded. Accounting for the effects of field length on soil loss is extremely important because this is one of the variables that land managers can manipulate. While the WEQ model (Woodruff and Sid-doway, 1965) uses an empirical method to account for field fetch effects, updating the soil surface provides a physically based approach.

The bare, crusted surfaces were somewhat more erodible than the bare, aggregated surfaces. Several factors contributed to this result. The rainfall reduced the random roughness of the aggregated surface, so initial soil saltation transport capacity was higher than on the aggregated surface. The initial reservoir of mobile abraded on the crust was increased downwind by abrasion. The abrasion then caused penetration of the downwind crust, thus exposing the additional reservoir of mobile soil aggregates below the crust. The final crust cover

Table 4. Soil loss simulation results (all values in kg m⁻²).

Field Length (m)	Max. Wind Middle					Max. Wind First, Aggregated Surface	Max. Wind Last, Aggregated Surface
	Aggregated Surface	Crusted Surface	Aggregated and Flat Residue	Crusted and Flat Residue	No Surface Update Aggregated		
Fine sandy loam							
800	4.52	5.96	1.26	2.01	5.17	3.81	4.67
400	2.11	5.64	0.54	1.14	5.61	2.14	2.62
200	0.76	3.51	0.22	0.43	6.37	1.15	0.96
100	0.23	0.73	0.10	0.16	7.00	0.51	0.26
Silt loam							
800	1.87	3.32	0.45	0.51	2.57	1.91	2.33
400	0.64	1.84	0.17	0.17	2.65	1.07	0.96
200	0.21	0.56	0.08	0.07	2.56	0.46	0.25
100	0.07	0.18	0.05	0.04	2.22	0.18	0.09

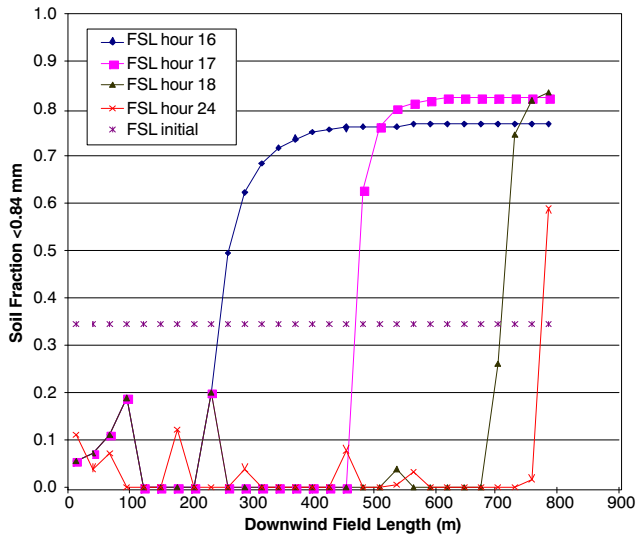


Figure 6. Changes in downwind surface mobile mass fraction (<0.84 mm diameter) during simulated wind storm (max. wind middle) on fine sandy loam soil (FSL).

fraction on the bare, fine sandy loam was reduced from the initial 0.97 to an average of 0.59 in the upwind 220 m and zero thereafter. On the silt loam, some crust remained over the entire surface, and the cover fraction averaged 0.52 at the end of the windstorm. The simulated windstorm was of long duration, and this also contributed to excessive destruction of the crusts. The frequent use of rolling harrows (sand fighters) by land managers on crusted sandy loam soils, however, attests to their increase in erodibility upon crusting.

As silt content increases, crusts are easily formed, but whether a crusted surface is more or less erodible than aggregated surfaces depends largely on the amount of crust destruction by abrasion (Chepil and Woodruff, 1963). Thus, crusts have low erodibility when they are formed by processes such as snowmelt or soil puddling that leave little or no mobile material on the surface. Crusts formed by rainfall

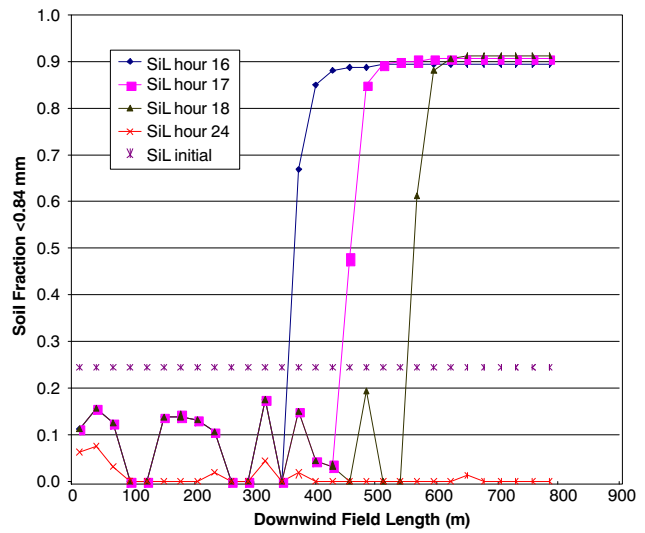


Figure 7. Changes in surface mobile soil mass fraction (<0.84 mm diameter) during simulated wind storm (max. wind middle) on aggregated silt loam soil (SiL).

often have less mobile material on the surface than similar aggregated surfaces (Chepil, 1951; Potter, 1990). Thus, combined with other erosion control measures such as trapping of abraded by surface roughness, protection by residues, or a short field length, crusts may remain largely intact and successfully limit the supply of erodible soil even in long-duration storms.

Modifying the storm wind speed distribution on the aggregated surface had mixed results (table 4). On the longest fields, soil loss increased when the highest wind speed was at the end of the storm because the downwind surface still had a large supply of mobile soil. This tendency is illustrated in figures 6 and 7 for the symmetric wind storms on the aggregated surfaces. While the silt loam surface was largely stable at the end of the high wind speed in hour 18, the downwind end of the fine sandy loam still had substantial mobile cover.

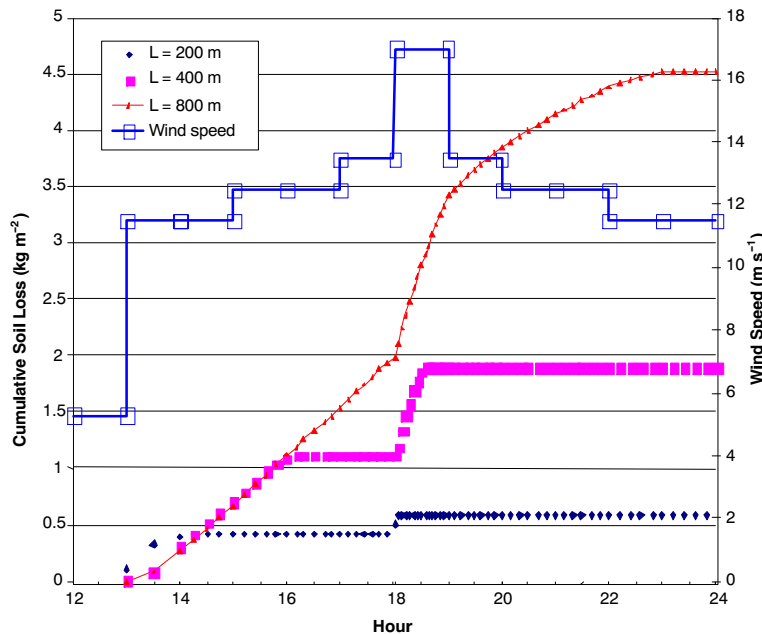


Figure 8. Simulated cumulative soil loss during simulated wind storm (max. wind middle) on aggregated, fine sandy loam soil.

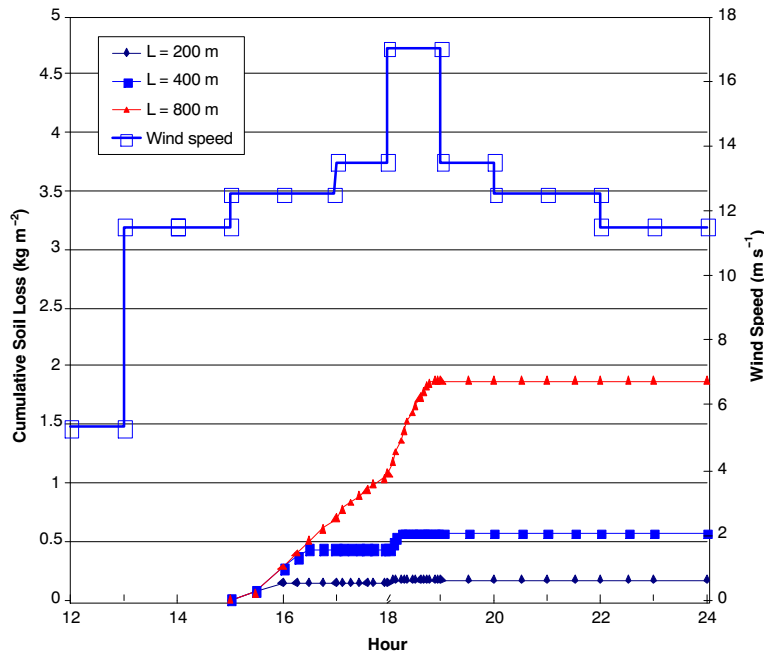


Figure 9. Simulated cumulative soil loss during symmetrical wind storm on aggregated, silt loam soil.

The results also illustrate that during storms with a short duration, there is often a substantial buildup of mobile soil on fields. This buildup frequently prompts land managers to undertake emergency tillage operations that increase surface roughness and create furrows to trap the mobile soil in order to reduce erosion in subsequent storms.

Simulating the aggregated surface without updating during the long-duration storm resulted in predicted soil losses significantly greater than that from the updated surfaces for two reasons (table 4). As the storm progressed, periodic updating resulted in increasing levels of surface cover of immobile clods that caused both intermittent erosion as wind speed

increased and, ultimately, stable, armored surfaces (figs. 8 and 9). Only the longest field with an aggregated surface continued to erode throughout most of the storm. The 400 and 200 m length fields stabilized after initial erosion and only lost additional soil when the wind speed was raised. They again stabilized at a new surface condition without further erosion after the peak wind speed. Part of the reason for the stabilization of the fields less than 800 m was that the reduction in random roughness was less than on the 800 m field (fig. 10). The point of minimum random roughness occurred where maximum simulated abrasion occurred on the field.

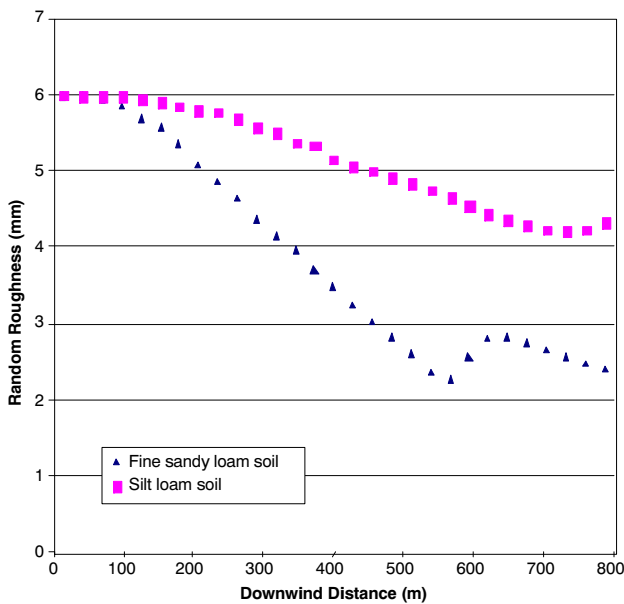


Figure 10. Simulated downwind random roughness at end of wind storm on aggregated surfaces of two soils with a uniform initial surface roughness of 6 mm.

CONCLUSIONS

This study shows that the net soil discharge and surface abrasion fluxes estimated by the WEPS model transport equations (Hagen et al., 1999) can be applied to simplified conservation of mass equations to update surface conditions in each grid cell on an eroding field. Further research is still needed to refine these surface update equations. Nevertheless, they currently enable WEPS users to simulate measured field erosion with good accuracy (Funk et al., 2004; Hagen, 2004). Further, the update equations enable WEPS users to simulate important observed erosion phenomenon. These include distinguishing between supply limited and unlimited conditions as influenced by field scale, erosive storm duration, and penetration of crusts by abraded. Estimating supply-limited conditions contributed to improving model accuracy. The update equations also enable direct simulation of field-scale fetch effects, and the durability of protective clods, crusts, and surface roughness. Estimating erosion effects on surface immobile elements as well as the buildup of mobile soil on downwind surfaces at the end of storms allows model users to judge the need for immediate control measures, such as emergency tillage, and to improve their designs of future erosion control systems.

REFERENCES

- Chepil, W. S. 1946. Dynamics of wind erosion: V. Cumulative intensity of soil drifting across eroding fields. *Soil Sci.* 61(3): 257-263.
- Chepil, W. S. 1951. Properties of soil which influence wind erosion: IV. State of dry aggregate structure. *Soil Sci.* 72(5): 387-401.
- Chepil, W. S. 1958. Soil conditions that influence wind erosion. Tech. Bull. 1185. Washington, D.C.: USDA-ARS.
- Chepil, W. S., and N. P. Woodruff. 1963. The physics of wind erosion and its control. *Adv. in Agron.* 15: 211-302.
- Fryrear, D. W., A. Saleh, and J. D. Bilbro. 1998. A single-event wind erosion model. *Trans. ASAE* 41(5): 1369-1374.
- Funk, R., E. L. Skidmore, and L. J. Hagen. 2004. Comparison of wind erosion measurements in Germany with simulated losses by WEPS. *Environ. Software and Modeling* 19(2): 177-183.
- Gillette, D. A. 1982. Threshold velocities for wind erosion on natural terrestrial surfaces (a summary). In *Precipitation Scavenging, Dry Deposition and Resuspension*, 1047-1057. H. R. Pruppacher, R. G. Semonin, and W. G. N. Slinn, eds. New York, N.Y.: Elsevier Science.
- Gillette, D. A., and W. Chen. 2001. Particle production and aeolian transport from a "supply limited" source in the Chihuahuan desert, New Mexico, United States. *J. Geophys. Res.* 106(D6): 5267-5278.
- Gillette, D. A., G. Herbert, P. H. Stockton, and P. R. Owen. 1996. Causes of the fetch effect in wind erosion. *Earth Surf. Proc. and Landforms* 21(7): 641-659.
- Gillette, D. A., T. Niemeier, and P. Helm. 2001. Supply-limited horizontal sand drift at an ephemeral crusted, unvegetated, saline playa. *J. Geophys. Res.* 106(D16): 18085-18098.
- Goossens, D. 2004. Effect of soil crusting on the emission and transport of wind-eroded sediment: Field measurements on loamy sandy soil. *Geomorphology* 58: 145-160.
- Hagen, L. J. 1991a. A wind erosion prediction system to meet user needs. *J. Soil Water Cons.* 46(2): 105-111.
- Hagen, L. J. 1991b. Wind erosion mechanics: Abrasion of aggregated soil. *Trans. ASAE* 34(4): 831-837.
- Hagen, L. J. 2004. Evaluation of the Wind Erosion Prediction System (WEPS) erosion submodel on cropland fields. *Environ. Software and Modeling* 19(2): 171-176.
- Hagen, L. J., E. L. Skidmore, and A. Saleh. 1992. Wind erosion: Prediction of aggregate abrasion coefficients. *Trans. ASAE* 35(6): 1847-1850.
- Hagen, L. J., L. E. Wagner, and E. L. Skidmore. 1999. Analytical solutions and sensitivity analyses for sediment transport in WEPS. *Trans. ASAE* 42(6): 1715-1721.
- Langston, G., and C. Mckenna Neuman. 2005. An experimental study on the susceptibility of crusted surfaces to wind erosion: A comparison of the strength properties of biotic and salt crusts. *Geomorphology* 72: 40-53.
- Lyles, L., and J. Tataro. 1986. Wind erosion effects on soil texture and organic matter. *J. Soil Water Cons.* 41(3): 191-193.
- Mansell, G. E., S. Lau, J. Russel, and M. Omary. 2006. Final report: Fugitive wind blown dust emissions and model performance evaluation: Phase II. Report prepared for Western Governors Association. Novato, Cal.: Environ International Corp.
- Okin, G., and D. A. Gillette. 2004. Modelling wind erosion and dust emission on vegetated surfaces. In *Spatial Modeling of the Terrestrial Environment*, 137-156. R. J. Kelly, N. A. Drake, and S. L. Barr, eds. New York, N.Y.: John Wiley and Sons.
- Potter, K. N. 1990. Estimating wind-erodible materials on newly crusted soils. *Soil Sci.* 150(5): 771-776.
- Skidmore, E. L., and J. B. Layton. 1992. Dry soil aggregate stability as influenced by selected soil properties. *SSSA J.* 56(1): 557-561.
- Stout, J. E., and T. Z. Zobeck. 1997. Intermittent saltation. *Sedimentology* 44(5): 959-970.
- Wagner, L. E., and L. J. Hagen. 2001. Application of WEPS-generated soil loss components to assess off-site impacts. In *Sustaining the Global Farm: Proc. 10th Intl. Soil Conservation Organization Conference*, 935-939. D. E. Stott, R. H. Mohtar, and G. C. Steinhardt, eds. West Lafayette, Ind.: Purdue University and USDA-ARS National Soil Erosion Research Laboratory.
- Woodruff, N. P., and F. Siddoway. 1965. A wind erosion equation. *SSSA Proc.* 29(5): 602-608.
- Zobeck, T. M. 1991. Abrasion of crusted soils: Influence of abrader flux and soil properties. *SSSA J.* 55(4): 1091-1097.

